Whole-Body FDG-PET Imaging for Staging of Hodgkin's Disease and Lymphoma

Carl K. Hoh, John Glaspy, Peter Rosen, Magnus Dahlbom, Shay J. Lee, Lori Kunkel, Randall A. Hawkin, Jamshid Maddahi and Michael E. Phelps

Divisions of Nuclear Medicine and Biophysics, Hematology and Oncology, Departments of Molecular and Medical Pharmacology, Radiology and Medicine, Laboratory of Biochemical and Environmental Sciences, The Crump Institute of Biological Imaging; UCLA School of Medicine; and UCSF School of Medicine, Los Angeles, California

Accurate staging of Hodgkin's disease (HD) and non-Hodgkin's lymphoma (NHL) is important for treatment management. In this study, the utility of 2-[^{18}F]fluoro-2-deoxy-D-glucose (FDG) whole-body PET was evaluated as an imaging modality for initial staging or restaging of 7 HD and 11 NHL patients. **Methods:** Whole-body PET-based staging results were compared to the patient's clinical stage based on conventional staging studies, which included combinations of CT of the chest, abdomen and pelvis, MRI scans, gallium scans, lymphangiograms, staging laparatomies and bone scans. **Results:** Accurate staging was performed in 17 of 18 patients using a whole-body PET-based staging algorithm compared to the conventional staging algorithm in 15 of 18 patients. In 5 of 18 patients, whole-body PET-based staging showed additional lesions not detected by conventional staging modalities, whereas conventional staging demonstrated additional lesions in 4 of 18 patients not detected by whole-body PET. The total cost of conventional staging was $66,292 for 16 CT chest scans, 16 CT abdominal/pelvis scans, three limited MRI scans, four bone scans, five gallium scans, two laparotomies and one lymphangiogram. In contrast, scans cost $36,250 for 18 whole-body PET studies and additional selected correlative studies: one plain film radiograph, one limited CT, one bone marrow scan, one upper GI and one endoscopy. **Conclusion:** A whole-body FDG-PET-based staging algorithm may be an accurate and cost-effective method for staging or restaging HD and NHL.

Key Words: whole-body PET; lymphoma; Hodgkin's disease; non-Hodgkin's lymphoma

J Nucl Med 1997; 38:343–348

The incidence of Hodgkin's disease (HD) and non-Hodgkin's lymphoma (NHL) is less than 8% of all malignancies. However, in men aged 15–54 yr, they are the third and second leading cause of cancer deaths in the U.S. (*1*). Fortunately, HD and NHL are also among the few malignancies that are potentially curable with current existing treatment modalities, even in advanced or recurrent disease.

The accurate staging of HD allows optimum selection of treatment options and results in improved treatment outcomes. The anatomic extent of disease is the single most important factor influencing relapse-free and total survival of patients with HD (*2*). In addition to clinical history and physical examination, the conventional methods for staging HD and NHL may include chest radiograph, CT or MRI of the neck, chest, abdomen, pelvis, bone scan, gallium scan, liver-spleen scan, lymphangiogram and laparotomy. Although whole-body scintigraphy with ^{67}Ga-citrate has been clinically useful in the staging of lymphoma, several reports have demonstrated a potential role of imaging lymphoma with 2-[^{18}F]fluoro-2-deoxy-D-glucose (FDG) (*3–6*). However, no prior studies have been published on the staging of HD and NHL with whole-body PET with FDG. The capability to accurately stage the entire body in a single imaging study would be clinically valuable, especially in patients in whom the anatomical distribution of disease recurrence is not predictable.

Tomographic images generally have higher contrast and sensitivity for lesion detection than similar nontomographic images. This principle holds not only for x-ray CT but also for SPECT and whole-body PET images (*7*). The whole-body PET technique acquires multiple image sets along the full length of the patient's body in a single acquisition session, and can display these images in tomographic transaxial, coronal or sagittal planes (*8,9*). In this study, we prospectively compared the accuracy of lesion detectability and anatomical staging and the cost of whole-body PET relative to the conventional staging work-up for lymphoma and HD.

MATERIALS AND METHODS

Patients

The referring oncologists recruited patients with a diagnosis of HD or lymphoma who needed a staging or restaging work-up. Informed consent, in accordance with the policies of the UCLA Human Subject Protection Committee, was required of all study participants as well as permission to release their medical records for clinical follow-up.

Clinical records were reviewed of 18 patients (7 men, 11 women; age range 17–70 yr, mean 46 ± 14 yr) for whom the anatomical extent of disease was later confirmed by biopsies or follow-up studies. Three patients had additional FDG whole-body studies at later dates. In most patients, other imaging modalities such as CT of the chest, abdomen and pelvis, standard ^{99m}Tc-methylenediphosphonate (MDP) bone scans and MRI were available as well as follow-up studies, which were used to ensure a more accurate assessment of the initial imaging studies.

Study Design

Patients had a whole-body PET study after completion of conventional staging tests that were selected by the oncologist (Fig. 1). The conventional imaging studies were mainly performed at a single institution. CT scans were obtained using conventional techniques for body imaging. For the chest images, 10-mm axial contiguous sections were obtained through the upper and lower thorax and 5-mm axial contiguous sections were obtained through the hila. Most studies were performed with oral and intravenous contrast. MR scans were performed with at least two sequences including T1 and T2 axial images and T1 coronal and sagittal images. The conventional staging test results were interpreted by an experienced radiologist. The radiologists had access to all

Received Mar. 7, 1996; revision accepted Jul. 19, 1996.

For correspondence or reprints contact: Carl K. Hoh, MD, UCLA School of Medicine, Division of Nuclear Medicine and Biophysics, CHS AR-128, 10833 LeConte Ave., Los Angeles, CA 90095-6942.

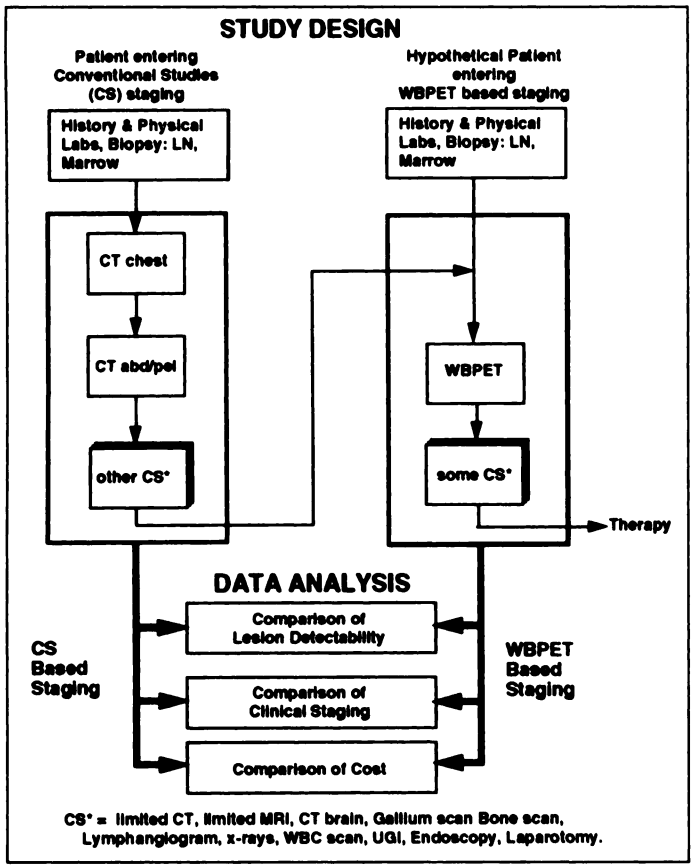

FIGURE 1. Study design to simulate hypothetical whole-body PET staging algorthim after completion of conventional staging costs and lesion detectability, clinical staging and total cost.

correlative results and information up to the date of that particular study. In addition, the whole-body PET studies were initially read unblinded to the conventional imaging results so that any discrepancies that would alter clinical management could be pursued with additional testing and also allow possible confirmation of positive whole-body PET findings that were negative on the initial conventional images.

PET Imaging

All patients fasted (except for water) for at least 6 hr before imaging. Patients were given an intravenous bolus injection of 10 mCi (370 mBq) sterile [^{18}F]FDG. The labeling of 2-deoxyglucose as described by Barrio et al. (*9*) provided the positron-emitting form of the glucose analog. Imaging was initiated after a 30-min uptake period. All patients were imaged without an indwelling urinary catheter.

Patients were studied on a whole-body eight-ring system that produces 15 simultaneous transaxial image slices per bed position. Eight interlaced bed positions were acquired that covered an 81-cm total axial field of view over the patient's upper body (typically spanning from the top of the head to upper pelvis). A second eight-bed interlaced acquisition was performed on the lower portion of the patient's body (typically covering the upper pelvis to the distal tibial level) after the patient voided. Total imaging time was 64 min. Images were reconstructed without attenuation correction into (192 × 192) transaxial images using a standard 0.30 Shepp-Logan filter, which gave a final image resolution of 10.1 mm (*8*). The transaxial images were then resliced into 32 tomographic coronal and 32 sagittal images. In addition, a set of two-dimensional projection images were formed by resorting the raw sinogram data into 32 nontomographic whole-body images that could be displayed as a rotating body on the computer (*8*).

TABLE 1
Average Cost of Diagnostic Procedures from Five Local Hospitals

Procedure	Cost
PET	$1900
Chest CT	$1100
Abdomen and pelvis CT	$1900
Brain CT	$1100
Limited CT	$ 850
Limited MRI	$1500
Plain film Xrays	$ 200
Bone scan	$ 800
Gallium scan	$ 800
WBC scan	$1000
Marrow scan	$ 800
Lymphangiogram	$1392
Laparotomy	$3000
Upper GI	$ 600
Endoscopy	$1000

These two-dimensional projection images were not reconstructed, thereby eliminating the possibility of reconstruction artifacts.

Qualitative Image Analysis

Tomographic images in the transaxial, coronal and sagittal planes were visually analyzed on a high-resolution display. In addition, two-dimensonal projection images were used to differentiate between normal and abnormal bowel activity. An abnormal focus of FDG uptake was defined as focal activity relatively higher than that of surrounding tissue with no similar activity seen in the contralateral side of the body. The whole-body PET images were interpreted by three investigators blinded to the results of the any prior conventional staging studies or biopsy results. Images were scored as positive, indeterminate or negative for abnormal FDG activity on a patient and anatomical site basis (Fig. 1). For indeterminate whole-body PET findings, however, additional study results could be requested to assist in the interpretation. These additional studies were added to the total cost analysis of the whole-body PET-based imaging algorithm. Conventional staging results were based on the official imaging reports and other medical records.

Data Analysis

The true clinical stage of disease was based on the final overall clinical evaluation, which included all available data (biopsies, conventional staging and whole-body PET results) and all follow-up studies and tests, which allowed confirmation of initial conventional staging and whole-body PET findings as they became apparant with time.

For the analysis of lesion detectability, each patient's imaging results from conventional staging or whole-body PET were tabulated into anatomical sites: cervical, supraclavicular, axillary, mediastinal, hilar, lung parenchyma, renal, periarotic, abdominal/pelvic, spleen, iliac, inguinal, bone and bone marrow. Each positive site of disease was scored as a unit increment in that anatomical site. This approach eliminated counting every discrete lesion within an involved anatomical site.

The staging accuracy for conventional staging compared to whole-body PET algorithms was performed by comparing concordance or discordance in overall numerical staging of disease between each patient.

The total costs for the studies ordered in the conventional algorithm were compared to the total costs of studies ordered in the hypothetical whole-body PET algorithm. The price for each conventional diagnostic procedure was averaged from five local hospitals (see Table 1). Costs such as routine blood testing or other minor procedures were not included in the comparison.

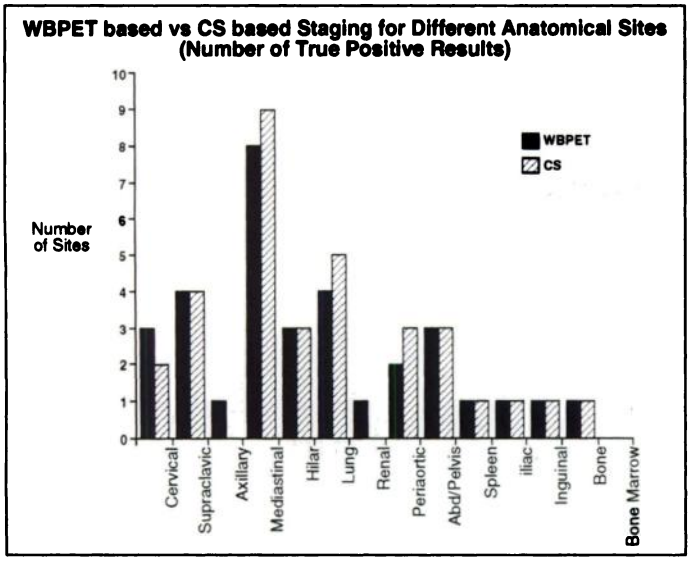

FIGURE 2. Whole-body PET and conventional staging algorithms found 33 of 37 disease sites. For both algorithms, undetected lesions (false-negatives) were different sites.

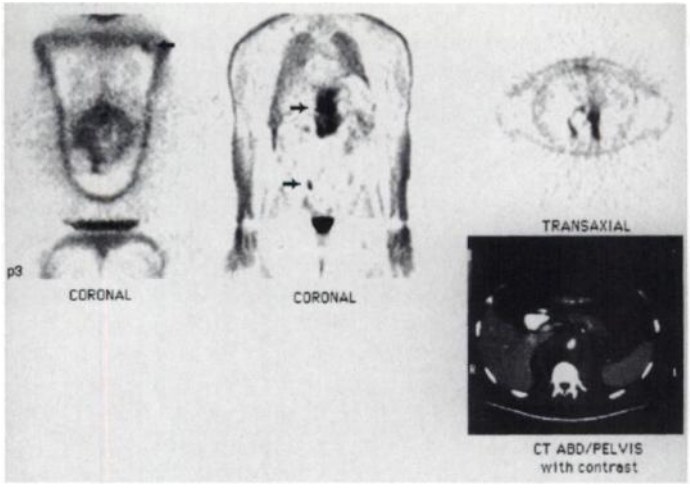

FIGURE 4. Coronal (p18), transaxial (p3, bed6) whole-body FDG images demonstrate a large complex mass in the upper abdomen with areas of hypermetabolism and ametabolism (necrosis) that correlate with the mass seen on the CT scan of the abdomen/pelvis. The coronal image shows a more accessible left axillary nodal focus where subsequent biopsy revealed a diagnosis of Burkitt's lymphoma.

RESULTS

Lesion Detectability

Thirty-seven positive disease sites were found based on biopsy (n = 8) or follow-up clinical assessment (n = 29) in the 18 study patients. Distribution of these sites and a comparision of the number of lesions detected by the whole-body PET algorithm compared to the conventional staging algorithm are shown in Figure 2. The whole-body PET and conventional staging algorithms detected 33 of 37 disease sites, although not all detected sites were the same. Whole-body PET staging found additional lesions not detected by conventional staging in the cervical area in Patient 8 with HD, periaortic nodes in Patient 12 with NHL (Fig. 3), an axillary node in Patient 15 with Burkitt's lymphoma (Fig. 4) and persistant renal activity in Patient 9 with renal transplant lymphoma.

On the other hand, the conventional staging algorithm found additional disease sites not detected by whole-body PET. For example, small mediastinal nodes (approximately 1.0-cm) with nodular diffuse mixed-cell lymphoma were found in Patient 8. In Patient 10, small scattered bilateral lung parenchymal nodules with diffuse large-cell lymphoma were sited. In Patients 8 and 11, both with NHL, small periaortic nodes were located. These small nodes were believed to be tumor since they increased in size on follow-up CT scans.

The number of false-negative or false-positive disease sites detected by whole-body PET and conventional staging algorithms compared to clinical follow-up is shown in Figure 5. Both the PET-based and conventional staging algorithms failed to detect intra-abdominal periaortic lymph nodes in one patient. False-positive findings for whole-body PET occurred in Patient 11 whose tumor activity could not be excluded due to physiologic bowel activity.

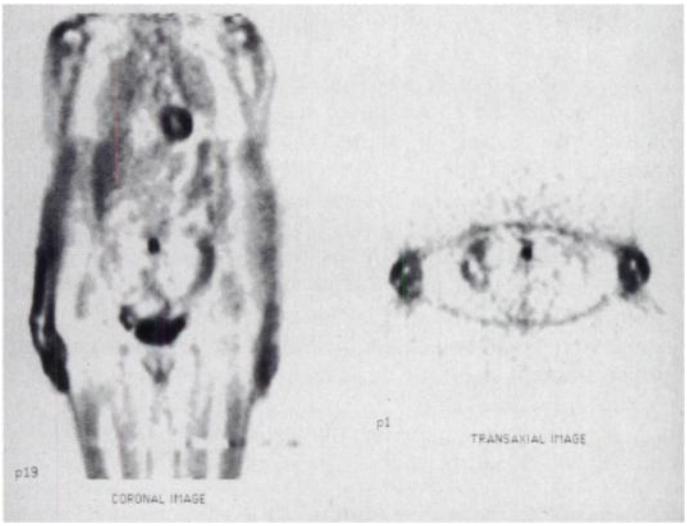

FIGURE 3. Coronal and transaxial whole-body FDG images in a patient with treated NHL. The patient was restaged and reported to have only a stable residual mass 1.5 × 2.5 cm in the left lower quadrant of the abdomen. Whole-body PET images show an intense focus of abnormal FDG activity in the periaortic region of the midabdomen consistent with the patient's recurrence of active disease.

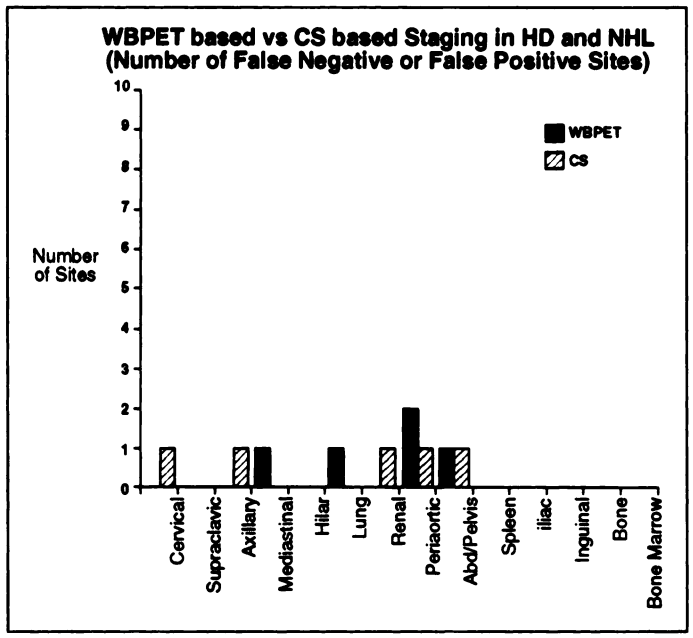

FIGURE 5. Comparison of the number of false-negative or false-positive disease sites based on the final clinical assessment. Whole-body PET staging failed to detected small scattered lung parenchymal lesions in a patient with NHL and small (~1.0 cm) nodes in the mediastinum and periaortic area in another patient with NHL. False-positive findings for whole-body PET occurred in one patient in whom tumor activity could not be excluded due to physiologic bowel activity.

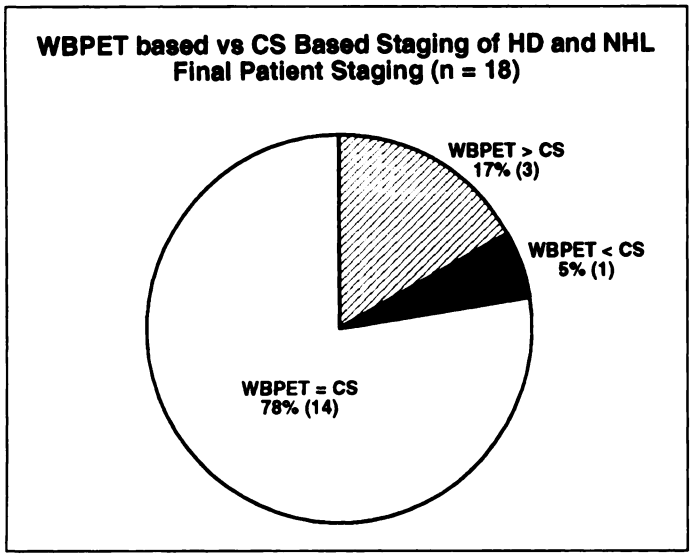

FIGURE 6. Comparison of clinical stage of disease for whole-body PET staging versus conventional staging. Whole-body PET algorithm correctly increased staging in three patients and incorrectly decreased staging in one patient.

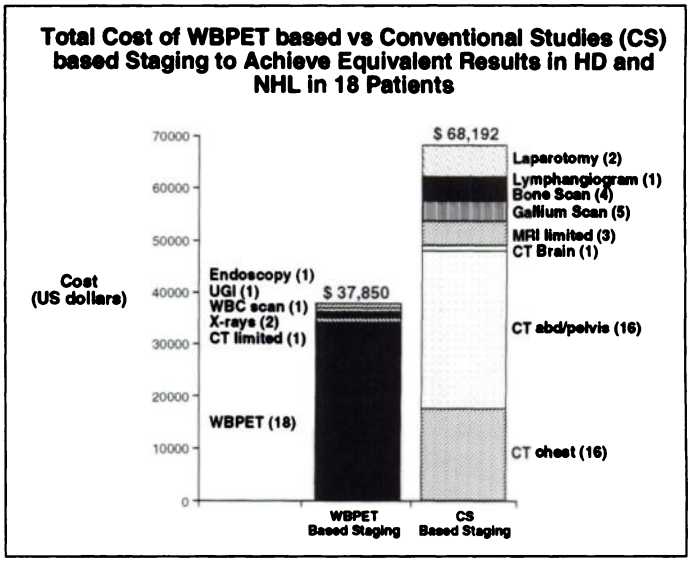

FIGURE 7. Cost comparisons of conventional and whole-body PET staging algorithms. Conventional staging costs 80% more than whole-body PET staging.

In two of the 18 patients, whole-body PET findings were scored as indeterminate, thereby requiring addtional studies to characterize the FDG activity. In Patient 3, increased FDG bone marrow activity was considered indeterminate. However, it was correctly catagorized in the whole-body PET based algorithm as benign reactive bone marrow based on a subsequent colloid bone marrow scan. In Patient 16, indeterminate activity in the left upper abdominal quadrant was found to be a lymphoma-infiltrated gastric ulcer by endoscopy.

Staging Comparison

A comparison of disease stage determined with the whole-body PET or the conventional staging algorithm is shown in Figure 6 and Table 2. For a particular anatomical site, disease detection or failure of detection may not necessarily change the overall tumor stage for that patient. In the whole-body PET algorithm, two patients (Patients 8 and 10) had false-negative sites of disease. In Patient 8, the mediastinum was one false-negative anatomical site and lymph nodes in the periaortic area were another. During follow-up asssesment 5 mo later, both sites were determined to be positive for disease based on increased lesion size on CT images. In Patient 10, bilateral scattered pulmonary nodules (<1.0 cm) consistent with lymphatic spread of disease were not detected by whole-body PET. In this NHL patient, the false-negative disease site would have incorrectly decreased the overall stage of disease.

In Patients 9, 15 and 16, the whole-body PET algorithm correctly increased the stage of disease. The anatomical sites of disease in these patients were a transplanted kidney, bilateral supraclavicular nodes and periaortic nodes, respectively.

Cost Comparisons

The total cost of the whole-body PET algorithm was $37,850 compared to $68,192 for the conventional staging algorithm of (Fig. 7). In the conventional staging algorithm, the major cost was for 33 CT scans, which included CT scans of the chest, abdomin and pelvis in 16 of 18 patients. Only two staging laparotomies were performed (~$3000 each), but they were a significant portion (~9%) of the total diagnostic conventional staging costs.

In the whole-body PET algorithm, additional imaging and diagnostic procedures were required to resolve indeterminate findings in two patients. In Patient 3, a plain film radiograph of the femur (~$200) and a bone marrow scan (~$800) were needed after the whole-body PET scan to resolve prominent bone marrow uptake of FDG in the bilateral femurs. One year later, bone marrow biopsy indicated a myleodysplastic syndrome as a result of the patient's chemotherapy. In Patient 16, focal FDG uptake on the left upper abdominal quadrant required an UGI barium study ($600), an upper endoscopy and a gastric biopsy ($1000), which revealed a lymphoma-infiltrated gastric ulcer.

DISCUSSION

In HD, the overall goal of staging is to cure the most patients with the least amount therapy to avoid complications. In intermediate and high-grade NHL, however, staging has limited importance in treatment planning relative to other prognostic factors (such as poor performance status, B symptoms, mass more than 10 cm, three or more extranodal sites, marrow involvement and LDH > 500). Staging is still extremely useful in defining the composition of NHL patients in clinical trials.

In this study, both the conventional staging and the whole-body PET staging algorithms correctly identified the same abnormal lesions sites in (31 of 37) lesion sites. The whole-body PET algorithm detected three additonal lesion sites that were missed in the conventional staging algorithm. However, conventional staging algorithm detected three lesions sites missed by whole-body PET. Both algorithms missed periaortic nodes in one patient. The lesions not detected by whole-body PET were small lesions in the lung parenchyma in a patient with NHL and ~1.0-cm nodes in the mediastinum and periaotic areas in another NHL patient. The significance of these missed lesions needs further study. The lesions missed by conventional staging were either outside the field of imaging (n = 1) or were not of sufficient size for catagorization as abnormal (n = 2).

Since the whole-body PET images in this study were performed without tissue attenuation correction, no estimation of tumor uptake could be made. The use of simultaneous transmission emission scans may allow more semiquantiative criteria for tumor uptake and, hopefully, more specificity in differentiating between tumor and nontumor uptake and estimating tumor response to therapy. Although absolute quantitation is not possible without proper tissue attenuation correction, the relative changes in FDG lymphoma activity measured by planar FDG imaging have been possible and appear to correlate with tumor

TABLE 2
Comparison of Imaging Test and Staging Results Based on Conventional Versus PET-Based Staging Algorithms

Patient no.	Age (yr)	Sex	Conventional staging			PET-based staging		
			Diagnosis	Stage	Required tests	Stage	Required tests	Confirmation
1	48	F	NS HD	IIIA	CT+	Same	PET+	FU+
2	17	M	NS HD	II	CT+, MRI+, BS−GA+	Same	PET+	BX+
3	46	M	NS HD	No disease	CT−	Same	PET+, MS+	BM−
4	27	F	NS HD	IIIA	CT+	Same	PET+	FU+
5	35	F	NS HD	IIIB	GA+, LAP+, LYM+	Same	PET+	BX+
6	70	F	HD	IIIA	CT+, GA+	Same	PET+	FU+
7	45	M	HD	IV	CT+, GA−	Same	PET+	FU+
8	55	F	IG NHL	III	CT+, MRI+, BS−	Same	PET+	FU+
9	45	M	IG NHL	No disease	US−	I	PET+	BX+
10	59	M	IG NHL	IV	CT+, GA+	II	PET+	FU+
11	33	F	LG NHL	II	CT+	Same	PET+	FU+
12	52	F	LG NHL	III	CT+	Same	PET+	FU+
13	59	M	HG NHL	No disease	CT−, BS−	Same	PET−	FU−
14	66	F	LG NHL	No disease	CT−, MRI−	Same	PET−	FU−
15	35	M	HG NHL	II	CT+	III	PET+	BX+
16	59	F	HG NHL	II	CT+	III	PET+	Gastric BX+
17	40	F	IG NHL	II	CT+	Same	PET+	FU+
18	31	F	IG NHL	I	CT+	Same	PET+	FU+

NS = nodular sclerosis; CT = computed tomography; MS = marrow scan; HD = Hodgkin's disease; GA = gallium scan; BM = bone marrow biopsy/aspiration; BS = bone scan; BX = biopsy; LG = low grade; MRI = magnetic resonance imaging; FU = clinical follow-up; IG = intermediate grade; LAP = laparotomy; HG = high grade; LYM = lymphangiogram; NHL = non-Hodgkin's lymphoma (Lymphocytic Lymphoma).

response (*5*). Theoretically, tomographic whole-body images have the advantage of excluding overlying soft-tissue uptake of FDG.

The whole-body PET algorithm was equal to the conventional algorithm in the staging of seven HD patients. In patients with NHL, the stage increased in three patients and decreased in one patient when the whole-body PET algorithm was used. The clinical significance of this when accurate staging in NHL is currently of limited importance, needs to be determined. A more practical application of whole-body PET may be to confirm relapse, especially when the site of recurrence is unsuspected, or to identify a more accessible tumor site for histological confirmation.

The results of this study indicate that whole-body PET based staging, when the initial whole-body PET scan guided further conventional diagnostic studies, is cost-effective compared to the current conventional staging algorithm. Even though a single whole-body PET scan is more expensive than other imaging modalities, whole-body PET may reduce the total cost of the staging work-up in patients with HD and in NHL by focusing the selection of anatomical imaging procedures only to the necessary regions. In the future, whole-body PET may be used for scanning soft-tissue tumor metastases, which is similar to the current application of ^{99m}Tc-MDP bone scans for the survey of skeletal metastases.

Study Limitations

Our patient population was small and nonuniform. Also, not all studies were performed at a single institution and not all lesions were histologically confirmed. Lastly, some lesions may have evolved during follow-up and were not actually present at the initial evaluation.

Several organs in the body can have physiologically normal but relatively intense FDG activity, which can pose problems in the detection of tumor lesions. The most notable region is the brain which normally consumes about 20% of ingested or injected glucose. Therefore, intense FDG uptake in this region may obscure a brain or CNS lesion. The heart will show intense FDG uptake if the patient is in a postprandial state. In this study protocol, as in other PET oncology imaging protocols, patients were required to fast to minimize myocardial uptake of glucose. The bowel wall is another organ that may have normal physiologic FDG uptake. This pattern, although irregular in shape and intensity can be relatively intense in uptake. Additionally, we displayed the original data in two-dimensional projection views, which was helpful in differentiating this activity from tumor. The intense FDG activity in the urine will also cause problems unless the bladder is drained or irrigated with a Foley catheter.

Despite the limitations of the study, there are some theoretical advantages of whole-body PET staging:

1. High lesion contrast and anatomical localization due to the tomographic images.
2. Lesion detection based on a biochemical signal rather than anatomical conventional staging.
3. A complete body survey in a disease with unpredictable recurrence. With the newer generation of whole-body PET scanners and the use of new three-dimensional data acquisitions, the sensitivity for lesion detection should be even better (*10*).

CONCLUSION

A staging algorithm based on whole-body FDG-PET and selected imaging tests may be an accurate and cost-effective method for staging HD and NHL.

ACKNOWLEDGMENTS

We thank Ron Sumida, Lawrence Pang, Fracine Aguilar, Der-Jenn Liu and Pricilla Conteras for their expert technical assistnace in performing the PET studies and Diane Martin for her artwork. The Crump Institute of Biomedical Imaging is operated for the U.S. Department of Energy by the University of California under contract no. DE-FCO3-87ER60615. This work was supported by the National Institutes of Health grants RO1-CA56655 and K08-

CA01669-03 by Whitaker Foundation Biomedical Engineering research grant.

REFERENCES

1. Boring C, Squires T, Tong T, Montgomery B. Cancer statistics. *CA Cancer J Clin* 1994;44:7–26.
2. Jotti G, Bonadonna G. Prognostic factors in Hodgkin's disease: implications for modern treatment. *Anticancer Res* 1988;8:749–760.
3. Okada J, Yoshikawa K, Imazeki K, et al. The use of FDG-PET in the detection and management of malignant lymphoma: correlation of uptake with prognosis. *J Nucl Med* 1991;32:686–691.
4. Okada J, Yoshikawa K, Itami M, et al. Positron emission tomography using [^{18}F]FDG in malignant lymphoma: a comparison with proliferative activity. *J Nucl Med* 1992;33:325–329.
5. Hoekstra O, Ossenkoppele G, Golding R, et al. Early treatment response in malignant lymphoma, as determined by planar [^{18}F]FDG scintigraphy. *J Nucl Med* 1993;34: 1706–1710.
6. Newman J, Francis I, Kaminski M, Wahl R. Imaging of lymphoma with PET with [^{18}F]FDG: correlation with CT. *Radiology* 1994;190:111–116.
7. Hoh C, Hawkins R, Dahlbom M, et al. Whole-body skeletal imaging with [^{18}F]fluoride ion and PET. *J Comput Assist Tomogr* 1993;17:34–41.
8. Dahlbom M, Hoffman EJ, Hoh CK, et al. Whole-body PET. I. Methods and performance characteristiconventional staging. *J Nucl Med* 1992;33:1191–1199.
9. Padgett H, Schmidt D, Luxen A, Bida G, Satyamurthy N, Barrio J. Computer-controlled radiochemical synthesis: a chemistry process control unit for the automated production of radiochemicals. *Appl Radiat Isot* 1989;40:433–445.
10. Cherry S, Dahlbom M, Hoffman E. Evaluation of a three-dimensional reconstruction algorithm for multislice PET scanners. *Phys Med Biol* 1992;37:779–790.

Technetium-99m-Tetrofosmin Whole-Body Scintigraphy in the Follow-up of Differentiated Thyroid Carcinoma

Peter Lind, Hans J. Gallowitsch, Werner Langsteger, Ewald Kresnik, Peter Mikosch and Iris Gomez
Department of Nuclear Medicine and Special Endocrinology, Landeskrankenhaus Klagenfurt; and Department of Internal Medicine, Barmherzige Brüder Hospital, Graz, Austria

The purpose of this study was to evaluate prospectively the reliability of the new nonspecific tumor-searching tracer tetrofosmin in the postoperative follow-up of differentiated thyroid carcinoma (DTC) during TSH suppressive thyroid hormone treatment. **Methods:** Whole-body scintigraphy was performed in 114 patients under TSH suppressive L-T4 treatment 20 min after intravenous injection of 370 MBq ^{99m}Tc-tetrofosmin by means of a dual-head gamma camera followed by three-dimensional SPECT in case of suspicious tracer uptake. The results of serum thyroglobulin, ultrasonography of the neck, ^{131}I whole-body scintigraphy, chest radiograph, transmission CT or MRI, and bone scintigraphy were also available. **Results:** A group of 68 patients without thyroid remnants who were tumor free and had no history of metastases or tumor recurrence showed a negative ^{99m}Tc-tetrofosmin whole-body scan. Another 24 patients (papillary carcinoma pT1N0M0) were also in complete remission, but had sonographically proven remnants (echonormal). Sixteen of them (67%) exhibited ^{99m}Tc-tetrofosmin accumulation in the thyroid bed, which corresponded excellently to the localization of the remnant. The third group comprises seven cases of local recurrence confirmed by histopathology after reoperation or by cytology after fine-needle aspiration where tetrofosmin scintigraphy clearly revealed relapse of malignancy in all cases. A total of 17 patients had distant metastases (11 pulmonary, 3 bone, 2 bone and pulmonary, 1 bone and soft tissue) discovered by different modalities, resulting in 44 lesions to be evaluated. Of the 23 radioiodine negative metastases, 17 were detected by tetrofosmin (74%), whereas all 21 radioiodine accumulating lesions also showed tetrofosmin positive scans. The overall sensitivity of ^{99m}Tc-tetrofosmin in detecting distant metastatic lesions was 86%. Four additional cases with radioiodine-negative disseminated lung metastases showed diffuse pulmonary tetrofosmin uptake. **Conclusion:** Technetium-99m-tetrofosmin is a promising tracer to detect malignant recurrence and distant metastases in the follow-up of DTC without the necessity of thyroid hormone withdrawal.

Key Words: technetium-99m-tetrofosmin; whole-body scintigraphy; differentiated thyroid carcinoma

J Nucl Med 1997; 38:348–352

In the follow-up of differentiated thyroid carcinoma (DTC), ^{131}I whole-body scintigraphy and the measurement of thyroglobulin (Tg) have been well-established methods for many years. The value of nonspecific tumor searching radionuclides such as ^{201}Tl or tracers such as ^{99m}Tc-sestamibi is a controversial point in the literature. For ^{201}Tl, several authors found sensitivities ranging from 45% to 94% (*1–5*); similar sensitivities ranging from 43% to 93% are given for ^{99m}Tc-sestamibi (*6–10*).

When the new cationic complex tetrofosmin [1,2-bis-(bis[-2-ethoxyethyl) phosphino]ethane] was introduced, which had been primarily developed for myocardial perfusion scintigraphy, we decided to investigate whether this tracer was suitable as a tumor-searching agent. The most likely mechanism for cellular uptake is diffusion of the lipophilic cation across the sarcolemmal and mitochondrial membranes in response to electrical potential (*11*). Initial preliminary in vitro uptake studies in tumor cell lines were performed by Wolf et al. (*12*). Just like ^{99m}Tc-sestamibi, it is still not known how cellular tumor uptake and intracellular binding mechanisms work for ^{99m}Tc- tetrofosmin. However, several preliminary clinical studies have shown that ^{99m}Tc-tetrofosmin accumulates in viable tumor tissue, including thyroid, breast and lung cancer (*13–19*).

Encouraged by a patient with extremely elevated Tg (32.720 ng/ml) but a negative post-therapeutic ^{131}I whole-body scan, whose ^{99m}Tc-tetrofosmin whole-body scan showed multiple pulmonary and bone metastases with excellent image quality, we started a prospective study in 1994 using ^{99m}Tc-tetrofosmin whole-body scans in the follow-up of our DTC patients.

MATERIALS AND METHODS

From November 1994 to November 1995, 114 consecutive patients (87 women; age 24–82 yr; mean 53 yr; 27 men; age 34–86 yr; mean 56 yr) were investigated with ^{99m}Tc-tetrofosmin whole-body scintigraphy while under TSH suppressive thyroid hormone treatment in the follow-up of DTC. With the exception of papillary carcinoma pT1N0M0 (lobectomy or subtotal thyroidectomy without radioiodine ablation), all patients underwent total thyroidectomy followed by radioiodine ablation of the remnant with 2960-3700 MBq ^{131}I.

Histology revealed papillary carcinoma in 73 patients (64%) and

Received Jan. 24, 1996; revision accepted Jul. 22, 1996.
For correspondence or reprints contact: Peter Lind, MD, Dept. of Nuclear Medicine and Special Endocrinology, St.Veiterstraße 47, A-9020 Klagenfurt, Austria.